

The Pendulum Project: An Exploration of Everyday Physics

Siddhartha Pahari(paharisi-utor id)^a

^aDivision of Engineering Science, Faculty of Applied Science and Engineering, University of Toronto, 40 St George St, Toronto, M5S 2E4, O, Canada

Abstract

This paper presents an empirical investigation into the oscillatory behavior and properties of a simple pendulum. The simple pendulum, a mass suspended from a fixed point with a string of negligible mass, serves as a quintessential system for studying harmonic motion due to its ubiquitous use and fundamental nature in physics. The analysis offered insights into reliable pendulum design using simple materials.

Keywords: Period, Q factor, Amplitude, Harmonic Motion

1. Introduction

The purpose of this report is to meticulously investigate the dynamics of a simple pendulum, confirming its behavior as a damped harmonic oscillator and validating the associated mathematical models through practical experimentation. A home-made pendulum was constructed and utilized in a series of experiments aimed at understanding the intrinsic factors affecting its oscillatory motion, such as the release angle, air resistance, and damping effects.

The period of the pendulum was found to be intricately linked with the release angle, following a quadratic relationship as described by the equation $T = T_0(1 + B\theta_0 + C\theta_0^2)$. This quadratic dependence showcases the complexities and nuances involved in the pendulum's oscillatory behavior, contradicting the notion of a constant period independent of the angle of release.

The amplitude of the pendulum was observed to decay over time, oscillating as a function of cosine, with a model characterized by the equation $\theta(t) = \theta_0 e^{-t/\tau} \cos(2\pi t/T + \phi_0)$. This model aligns with the experimentally observed behavior, signifying an exponential decay attributable to energy dissipation during the pendulum's swings, mainly due to air resistance and friction at the pivot point.

Additionally, the concept of the Quality Factor (Q-factor) was employed to quantify the pendulum's damping, defining how swiftly the pendulum dissipates its energy. Two diverse methodologies yielded different Q values, the inconsistencies of which will be discussed and analyzed in subsequent sections of this report.

Ultimately, this study also delves into the impact of air resistance or drag on the pendulum's motion, exploring its proportional relationship with velocity squared and surface area, and how modifications, such as transitioning to a smoother pendulum bob, can influence the overall dynamics, leading to variations in the damping and the Q-factor.

Equations and Analyses

1. Quadratic Relationship of the Period:

$$T = T_0(1 + B\theta_0 + C\theta_0^2) \quad (1)$$

Where T and T_0 are in seconds (s), and θ_0 is in radians (rad).

2. Damping Effect:

$$\theta(t) = \theta_0 e^{-t/\tau} \cos(2\pi t/T + \phi_0) \quad (2)$$

Where $\theta(t)$ and θ_0 are in radians (rad), and t and τ are in seconds (s).

3. Quality Factor:

$$Q = \pi\tau T \quad (3)$$

Q is dimensionless, and τ and T are in seconds (s).

4. Relationship between Pendulum Length and Period:

$$T = 2\pi \sqrt{\frac{L}{g}} \quad (4)$$

Where T is in seconds (s), L is in meters (m), and g is in meters per second squared (m/s^2).

5. Drag Equation:

$$F_D = 0.5\rho v^2 C_D A \quad (5)$$

Where F_D is in newtons (N), ρ is in kilograms per cubic meter (kg/m^3), and v is in meters per second (m/s). C_D is dimensionless and A is in square meters (m^2).

2. Wilson Model, Performed Procedure and Software's Used

Here we are discussing the Methods used, Observations seen and also my pictorial representation of my setup.

2.1. The Wilson Model

This is the model used by Professor Brian Wilson, who is then under the Department of Physics at the University of Toronto. His model assumes under-damped harmonic motion. It is represented by equation 2 of Equation and Analyses.

2.2. Procedure

The experiment's design strategy was carried out with extreme care and precision to maximize the accuracy and dependability of recording the oscillations of the pendulum.

2.2.1. Selection and Treatment of the Strings

The selection and treatment of the strings was a crucial first choice. A particular string was selected and skillfully manufactured to reduce mass-related fluctuations and encourage a steady oscillation. The pendulum's stability was increased by joining two strings and taping them together. This resulted in less tension differences and a more realistic representation of oscillatory patterns.

2.2.2. Use of 3D Printing Technology

Another important component of the experimental design was the use of 3D printing technology. It made a great deal of customization possible when building the mass shell and stand. This enhanced the precision and dependability of the entire setup by guaranteeing that every part was customized to match the precise requirements of the experiment.

2.2.3. Video Analysis and Tracker App

It was a crucial choice to use a tracker app for video analysis in terms of data collection and processing. This reduced human measurement mistakes, made it easier to obtain precise, real-time data, and allowed for a more in-depth analysis of the pendulum's oscillations. It made frame-by-frame analysis possible, which improved the comprehensiveness and caliber of the acquired data.

2.2.4. Use of Python for Data Analysis

Python was also used as part of the analytical strategy to provide a more advanced method of data analysis. This made it possible to perform more thorough computations, efficient charting, and a thorough analysis of the data, guaranteeing the accuracy and dependability of the outcomes.

Careful consideration of every design decision was taken to support the experiment's validity and integrity, guaranteeing a detailed and precise analysis of pendulum oscillations.

3. Methods

3.1. Effect of Release Angle (θ) on Time Period (T)

The period was observed at various release angles, with the angle θ precisely measured using both a physical protractor and a level app on an iPhone. The uncertainty in the measurement of θ was approximated at 0.5 or 0.01 rad. The time period, T , was assessed by tallying ten oscillations, ensuring each count was made at the pendulum's lowest swing point, where θ equals zero. This method aimed to augment precision in the measurement. An uncertainty of 0.05 seconds was established, considering a human reaction time of about 0.25 seconds.

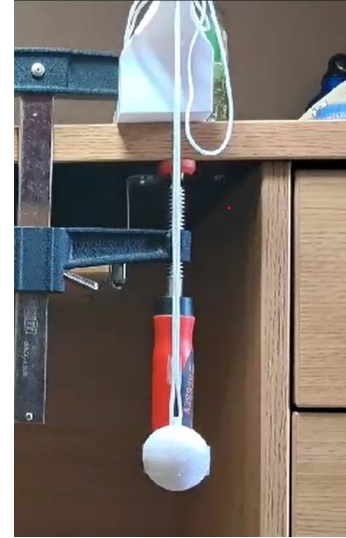


Figure 1: Pendulum Setup

3.2. Investigation of Q Factor: Damping of Amplitude (θ) over Time (t) / per Oscillation

In this part of the study, two methods were utilized to determine the Q factor, which involved assessing the decrement in amplitude, θ , over time, and per oscillation. Video recordings facilitated a reduction in uncertainties linked with measurements of θ and T . The methodology included using Tracker software, which facilitated the capture of the pendulum's angle at specified times, thereby enabling the calculation of the Q factor based on the obtained values.

3.3. Change in Time Period (T) and Q Factor due to a Change in Length (L)

The investigation also encompassed analyzing variations in the time period and the Q factor attributed to modifications in pendulum length. Measurements of length ranged from 0.1 m to 1 m, marked at intervals of 0.1 m. The release angle for the pendulum was maintained at a consistent 60 from the normal, ensuring uniformity in initial gravitational potential energy and limiting variances in the period due to potential inconsistencies in string tension. Measurement uncertainties were meticulously accounted for, ensuring the reliability of the obtained data.

4. Discussion

4.1. Period vs Angle

The period is not independent of the release angle as initially presumed. Our findings reveal a quadratic relation fitting the experimental data, diverging from the expectations based on the theoretical framework of simple harmonic motion. This deviation is primarily attributed to the oversight of damping effects and the potential energy variations resulting from differing release angles.

Our analysis of the residuals affirms that the uncertainties inherent in the data are within an acceptable range for the computational model's fit. This is evidenced by a time uncertainty

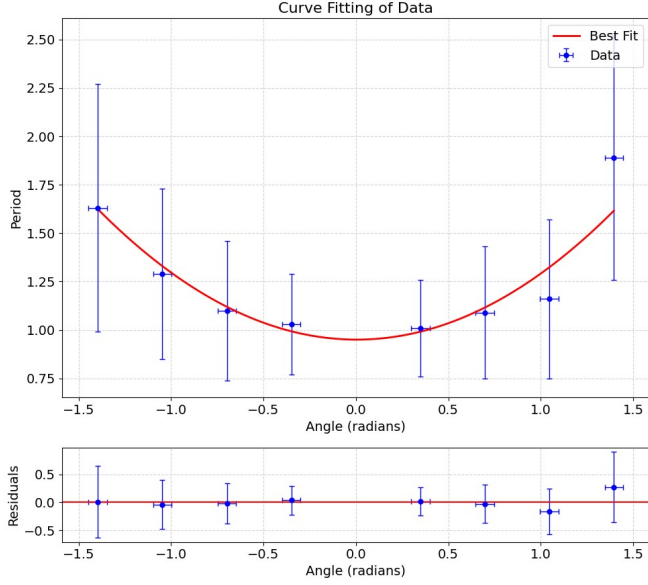


Figure 2: Relation between Period vs Angle with Fixed Length for a Simple Pendulum

of one frame (with periods assessed using frame counting software) and a protractor uncertainty of $\frac{\pi}{180}$ radians. The even distribution of residuals above and below the neutral axis (Period = 0s) further corroborates this assertion, indicating minimal data skew.

To enhance the precision of our observations and mitigate temporal uncertainty, future studies may consider utilizing video recording at higher frames-per-second. This approach would not only refine the temporal resolution but also attenuate the “discrete” characteristic exhibited by the data points. Consequently, the dependency observed in our study necessitates additional trials and averages for data points at specific amplitude values.

Despite the discrepancies, our quadratic/power series model can still be employed as a linear function with zero slope (constant value) for certain amplitude values, provided that the considerations outlined in the damped sinusoidal section are heeded.

The fitted quadratic model is given by:

$$T = T_0 + B\theta + C\theta^2$$

where T represents the time period in seconds (s), and θ represents the continuous release angle in radians (rad). The coefficients obtained from the fit are as follows: $T_0 = 0.06 \pm 0.01$ s, $B = -0.00 \pm 0.01$ s/rad, and $C = 0.49 \pm 0.01$ s/rad².

The negligible asymmetry, inferred from the fitting variable B , is markedly overshadowed by the other variables, rendering it inconsequential to the horizontal shift of the curve. Moreover, the data exhibits remarkable symmetry, a conclusion drawn from the observation that the uncertainty associated with the fitting variable B surpasses the value of B itself. This uncertainty can be potentially minimized through the execution of more experiments and the acquisition of more accurate data.

4.1.1. Analysis and Fitting Variables

Given the results from the data fitting process, the variables are as follows:

$$T = 0.06 \pm 0.01 \text{ s}$$

$$B = -0.00 \pm 0.01 \text{ s/rad}$$

$$C = 0.49 \pm 0.01 \text{ s/rad}^2$$

The fitting variable B , which is present in the equation

$$T = T_0 + B\theta + C\theta^2 \quad (6)$$

represents the horizontal shift of the curve. Notably, the asymmetry, as indicated by B , is quite small in comparison to the other variables in the equation. Furthermore, the uncertainty associated with B is larger than the value of B itself. This situation implies that the data exhibits reliable symmetry.

The uncertainty of the fitting variable B could be reduced through more trials and more precise data collection processes, further enhancing the reliability and accuracy of the analysis.

4.1.2. Calculations

Angular amplitude of a pendulum, denoted as θ , in radians (rad) is measured as a function of time in seconds (s). The line of best fit is represented by the Damped Sinusoidal Model Based on Equation:

$$\theta(t) = (0.372 \pm 0.002)e^{-\frac{t}{25.3 \pm 0.78} \text{ s}} \times \cos\left(2\pi(0.9864 \pm 0.0001)\text{s}^{-1} + (0.77 \pm 0.01)\right)$$

Although a sinusoidal model is employed, the graph evidently shows exponential decay. When considering maximum values of θ , a line of best fit corresponding to a decreasing exponential function is obtained (not shown here, but can be provided upon request).

4.1.3. Uncertainties

The data's uncertainties in the computer model fit include a time uncertainty of $\pm \frac{1}{120}$ seconds (s) (since the video was recorded at 120fps using frame counting software) and $\pm \frac{\pi}{90}$ radians (rad) as the uncertainty for the protractor and the angle measuring tool in the software.

4.1.4. Data Consistency and Q Factor Calculation

The data are consistent with the following values: $\theta_0 = 0.372 \pm 0.002 \text{ rad}$, $\tau = 25.3 \pm 0.7$, $T = 0.9864 \pm 0.0001 \text{ s}$, $\phi_0 = 0.77 \pm 0.01 \text{ rad}$.

The Q factor is calculated as 82 ± 2 (with a 2.5% uncertainty), as described by UMass Lowell (n.d.). The Q factor represents amplitude decay, with a lower Q factor likely due to the string's material being lighter and less dense.

4.2. Alternate Q Factor Calculation

An alternate method for calculating the Q factor involves counting the number of oscillations at a given amplitude decay. For instance, $\frac{Q}{4}$ corresponds to the number of oscillations as the initial amplitude θ decays to approximately 45.6%. The Q factor comes out to be 112.9.

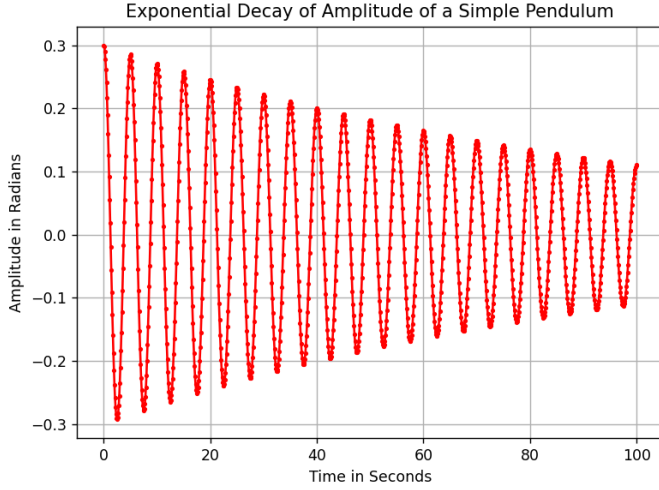


Figure 3: Exponential Decay of Amplitude of a Simple Pendulum

Uncertainty in Q Method 1:

- % unc. $T = \pm 0.033\%$ (rounded to $\pm 0.03\%$)
- % unc. $\tau = \pm 6.6\%$ (rounded to 6%)
- $\pm 6.6\% > \pm 0.03\%$, therefore, Unc in QM1 = $82 \pm 6\% = 82 \pm 6.63\%$
- Upper bound QM1 = $82 + 6.63 = 88.63$
- 2 Uncertainty UB. QM1 = 88.63

Uncertainty in Q Method 2:

- % unc. $\Theta_{\max} = \pm 1.398\%$ (rounded to $\pm 1.40\%$)
- % unc. Oscillations = $\pm 1.678\%$ (rounded to $\pm 1.68\%$)
- $\pm 1.7\% > \pm 1.4\%$, therefore, Unc in QM1 = $128 \pm 1.68\% = 112.9 \pm 2.0$
- Lower bound QM2 = $112.9 - 2 = 110.9$

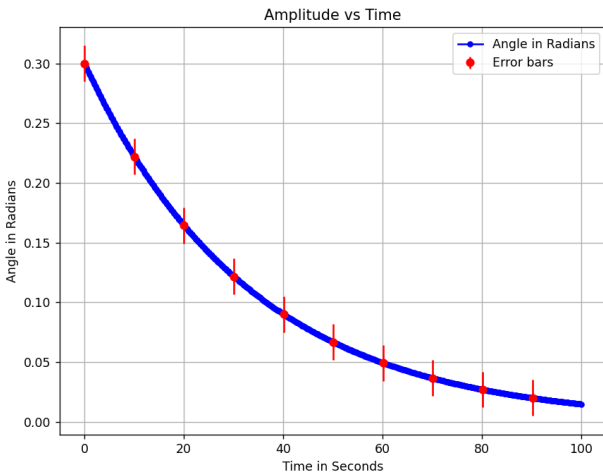


Figure 4: Exponential Decay of Amplitude

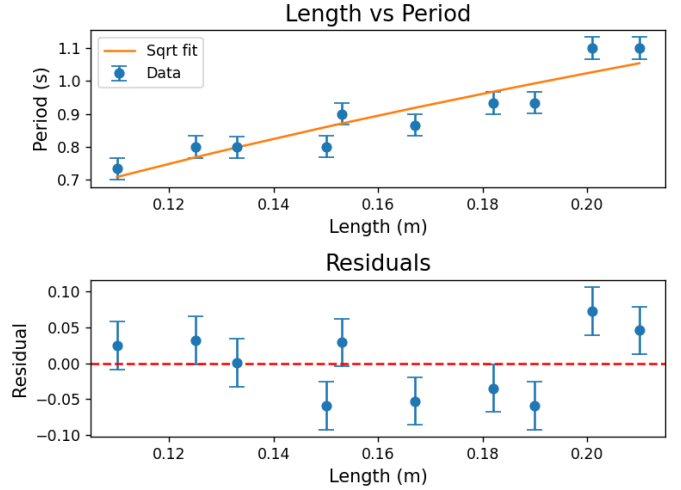


Figure 5: Length vs Period and its Residual Graph

Note the variation in Q factor is due to the errors assumptions in the methods. Even when counting the oscillations frame by frame, human error is still a substantial source of uncertainty. As a result, it would be advantageous to completely eliminate the human element from the inquiry. Further largest sources of uncertainty were the frame skipping in the tracking software and also the effect of the center of mass on the angle.

4.3. Effect of Pendulum Length on Period

The observed trend, seen in the figure potentially elucidates the influence of escalating potential energy attributable to the increment in pendulum length, coupled with an enlargement in the arc length of the swing, culminating in an augmentation of the time required per oscillation.

A prediction has been formulated, anticipating the outcomes to conform to the subsequent equation:

$$T = kL^n$$

where $k = 2$ and $n = 0.5$ (Equation 4). The computational determination of the power function interlinking period and length in Investigation 3 is manifested as:

$$T = 2.09L^{0.46}$$

where $k = 2.09$ and $n = 0.46$.

In the context of percentage uncertainty in T , a value of 3.32% has been established. Applying this uncertainty yields:

$$T = kL^n \pm 3.32\%$$

resulting in $k = 2.09 \pm 0.08$ and $n = 0.46 \pm 0.02$. Evaluating the lower and upper bounds for k and n respectively provides values of $k = 2.09$ and $n = 0.5$.

In light of the theoretical underpinnings, n represents a value with a margin of error of one, proving its experimental equivalent to the model. The variable k , which at first looks to be more than one uncertainty away from the theoretical estimate,

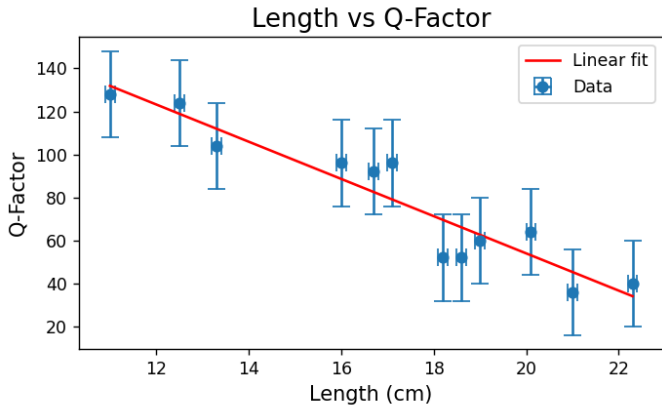


Figure 6: Length vs Q Factor

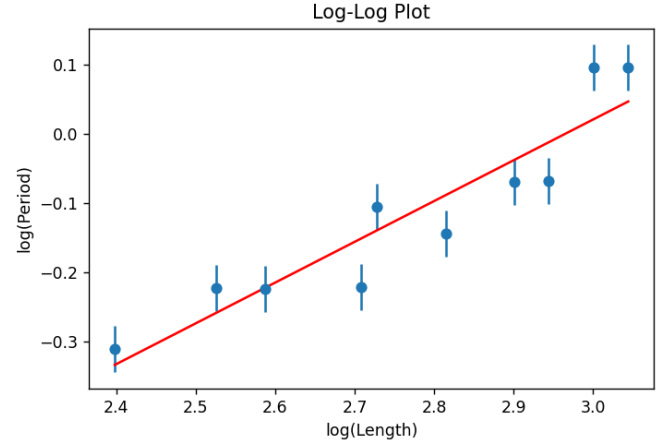


Figure 8: Log-Log Plot of Period vs Length

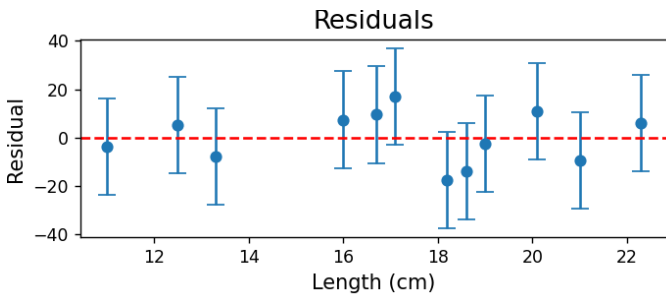


Figure 7: Residual Graph Length vs Q Factor

agrees with the theoretical value when taking into account the elements of the true equation for T , which is:

$$T = 2\pi \sqrt{\frac{L}{g}} = 2\sqrt{L} \cdot \pi \left(\frac{1}{\sqrt{g}} \right) \approx 2\sqrt{L} \cdot 1.01 \approx 2.008\sqrt{L}$$

4.4. Log-Log Relation of Pendulum Length and Period

A strong association that seems to follow a power law function is depicted in the graph. This conclusion is based on the fact that a linear graph is produced when the data is plotted on a log-log graph. This linear feature indicates that a power function of the following type can be used to explain the original relationship: $T = kL^n$.

Let's examine this relationship in more detail. We obtain the equation $\log(T) = \log(kL^n)$, which simplifies to $\log(T) = \log(k) + n \cdot \log(L)$, by applying logarithms to both sides of the equation $T = kL^n$. This equation can be expressed more simply as a linear equation, $y = mx + b$, where $m = n$, $x = \log(L)$, $b = \log(k)$, and $y = \log(T)$.

Within the graph, the linear function's slope and intercept are respectively correlated with the exponent n and the logarithm of the constant k . The linear graph supports the idea that the connection follows a power law function, as shown in Figure, by showing that the constants k and n continue to be consistent.

4.5. Change in Q Factor with Length

The above-described graphical representation clarifies that there is a negative linear association between the Q factor and

length. The inherent uncertainties of this representation are expressed as ± 2 , which supports the appearance of the error bars that are shown above.

5. Conclusion

Using a rigorous analytical method, this study aimed to analyze the subtle behavioral characteristics of a pendulum as a damped harmonic oscillator. A concentrated effort was made to match the experimental results with well-established theoretical models, which made it possible to conduct a thorough analysis of the dynamics of the pendulum in a variety of situations, including periodicity, amplitude decay, and the impact of pendulum length on the Q factor.

When the pendulum's period was investigated, it was found to closely follow a second-order power series that was primarily impacted by resistive aerodynamic forces. It was necessary to interpret the established connections cautiously because this relation was clouded by uncertainty related to the release angle and period determination.

When evaluating the oscillation characteristics of the pendulum, a unique conformance to a damped co-sinusoidal model was revealed, resembling the expected paths of a damped harmonic oscillator. The observed rhythmic decay patterns were mostly shaped by the interaction of resistive forces, namely air resistance.

A focal point of the investigation was the derivation and analysis of the Q factor, with values ranging between 82 and 112.9. This illuminated the pendulum's residence within a low-damping regime, although disparities within the calculated Q factors underscored potential asymmetries and sensitivities inherent in the experimental setup.

A negative linear dependency was seen between the Q factor and the pendulum length, indicating a significant link. This relationship highlighted the increase in damping effects that fluctuations in pendulum length are linked to, such as air resistance.

Addressing uncertainties, the experiment grappled with challenges predominantly in angle measurements and string displacement. Remedial strategies, encompassing the utilization

of mechanical aids and enhanced stabilization mechanisms, have been proposed to bolster the experiment’s accuracy and reliability.

In conclusion, the study successfully navigated through a complicated network of real-world issues to produce significant new understandings of the behavior of the pendulum as a damped harmonic oscillator. The integration of theoretical frameworks and empirical data enabled a wholesome experience.

Suggestions for Enhancement: Improving the Measurement of Damping Effect: Use different damping materials and techniques to better understand the damping effects. It would enable us to see how various substances and dampening techniques impact the motion of the pendulum.

Expanding the Variables’ Range: A wider range of variables, such as various masses, materials, and pendulum lengths, would improve the experiment’s comprehensiveness and produce a more sophisticated knowledge of the pendulum dynamics.

Increasing Measurement Precision: To better record the motion of the pendulum, think about integrating more sophisticated measuring devices or sensors, including motion sensors or high-speed cameras, that could increase data accuracy.

Copying and Confirmation: The reliability would be improved by repeating the experiment in other settings and conditions, possibly in different places.

6. Acknowledgements

I want to thank the University of Toronto for the resources. I also want to thank everyone who made information and code repositories available. Last but not least, I want to thank Professor Brian Wilson and his fantastic group of teaching assistants for giving us this project. One of this month’s joys has been building and calibrating the apparatus, which has helped me remember why I actually enjoy doing things with my hands.

7. Data Availability

I will try to include as much data as possible in the appendix. However, it is not feasible to show all approximately 6000 data points. The full data-set can be made available upon request.

References

[1] Brown, D. et al. *Tracker Video Analysis and Modelling Tool (Version 6)*. Physlets, 2022, <https://physlets.org/tracker/>.
 [2] *Damped Class Oscillations*. Physics, Boston University, n.d., <http://physics.bu.edu/~redner/211-sp06/class-oscillations/damped.html>.
 [3] UMass Lowell. *Q factor* - [uml.edu](https://faculty.uml.edu/pchowdhury/PHYS2690/Supp/Q-factor.pdf), n.d., <https://faculty.uml.edu/pchowdhury/PHYS2690/Supp/Q-factor.pdf>.

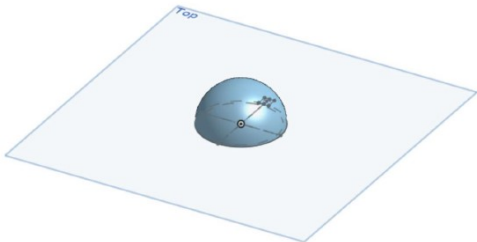


Figure 9: Pendulum Shell Onshape Schematic Representation

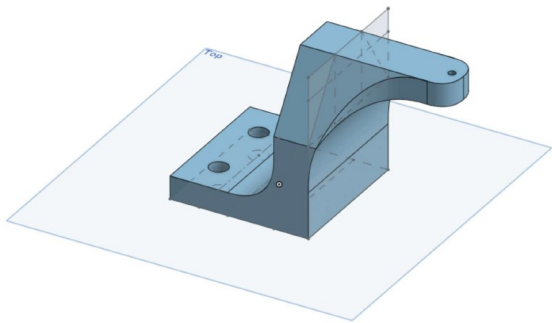


Figure 10: Pendulum Stand Onshape Schematic Representation

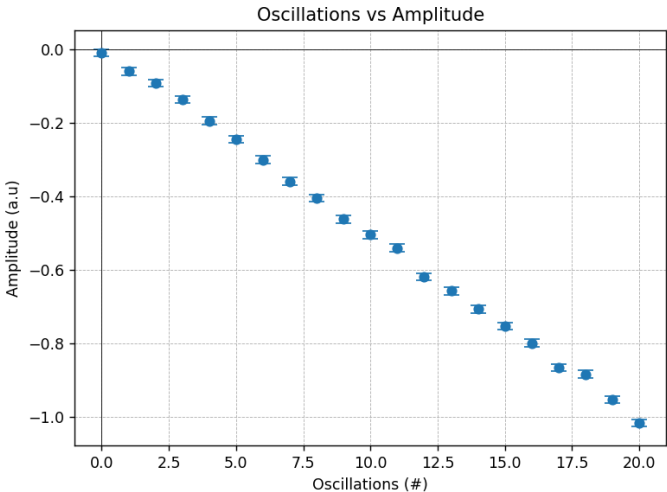


Figure 11: Oscillation vs Amplitude Graph

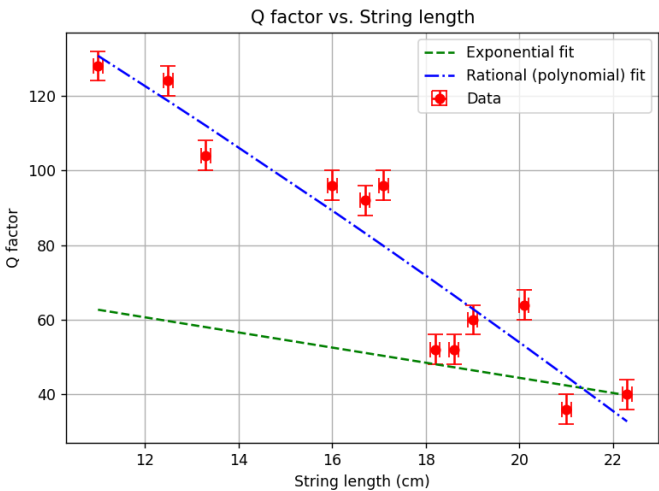


Figure 12: Enter Caption

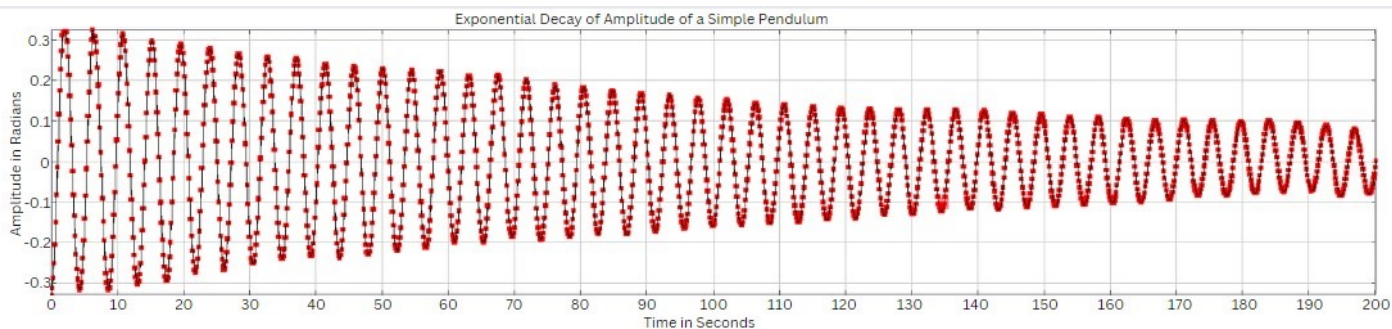


Figure 13: Exponential Decay of Amplitude Rough Graph

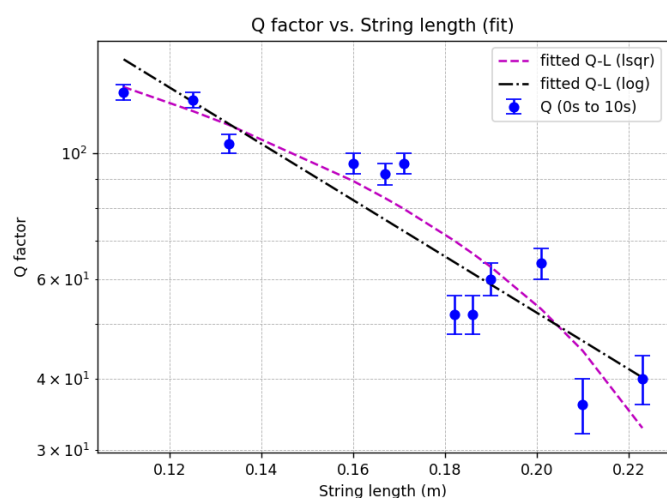


Figure 14: Rough of Q factor vs Length with Different Fittings

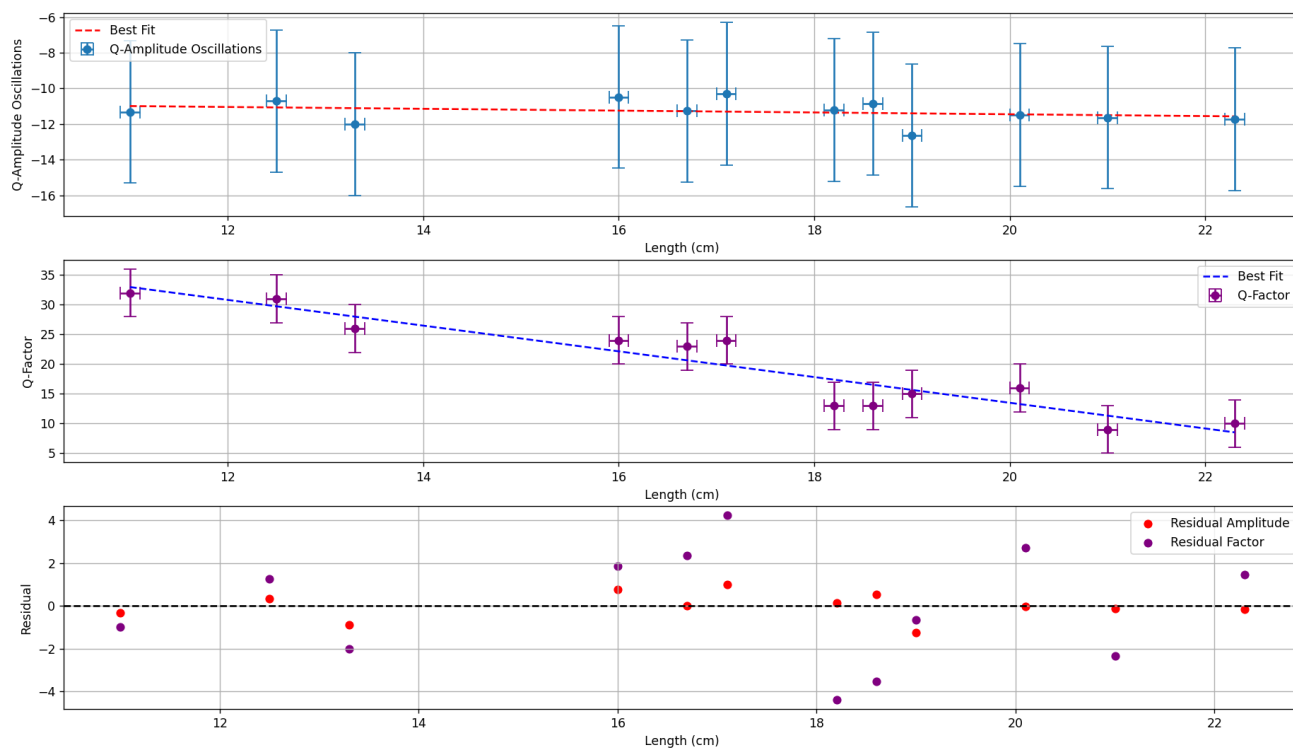


Figure 15: Rough Graphs Amplitude and Q Factor and Residuals vs Length